



# Investigation on the geometry of beams for piezoelectric energy harvester

E. L. Pradeesh<sup>1</sup> · S. Udhayakumar<sup>1</sup>

Received: 10 October 2018 / Accepted: 2 November 2018 / Published online: 14 November 2018  
© Springer-Verlag GmbH Germany, part of Springer Nature 2018

## Abstract

This paper presents various designs of the cantilever based piezoelectric energy harvester, which is excited using mechanical vibrations at the fixed end. By varying the geometries of the cantilever beam; higher stress, strain and consequently higher voltage and power could be attained from the same piezoelectric material. The analysis of energy harvesters were done using COMSOL Multiphysics 5.3a. The stress, strain and frequency response of the beams were verified by analytical, numerical and experimental methods. The result shows that the inverted taper in thick and width and inverted taper in width types of beams generated 47.39% and 21.31% more power compared to the rectangular cantilever beam. The resonant frequency of the inverted taper in thick and width beam is 53.3% less than the rectangle beam.

## 1 Introduction

Energy harvesting is the process of self-feeding power to run low power electronics devices. By using this method, the dependency of applications on batteries and external power sources can be eliminated. Vibration is the mechanical source of energy and piezoelectric material is used to convert mechanical energy into electrical energy.

Currently, wireless devices (Damy et al. 2018) gained more attention in the electronic devices; most of these devices are designed to run on batteries and external power sources. In remote areas, external power source availability is sparse. Due to the miniature size of the electronic devices, dismantling and assembling is difficult along with the frequent replacement of depleted batteries (Chandrakasan et al. 1998; Roundy and Wright 2004). To overcome this, an alternative method is energy harvesting. Mechanical vibration attracts the researchers as it is considered a potential source of power for the wireless and low power electronics devices (Md Ralib et al. 2011). Electromagnetic, electrostatic and piezoelectric generators are used to convert mechanical vibrations into electrical energy

(Roundy et al. 2003). Among these generators, piezoelectric has the capability to produce more energy density.

Geometrical factors of energy harvester have a significant effect on power production. The cantilever beam is mostly used in an energy harvester to place piezoelectric materials (Mossi et al. 2005). The ratio of the piezoelectric layer to the substrate has a significant effect on energy harvesting (Kim et al. 2005). By optimizing the geometry of the cantilever beam there is a chance to increase the power production of piezoelectric materials. Mateu and Moll (2005) analytically studied the strain on a rectangular and triangular cantilever beams. From the work, it could be inferred that the triangular beam has the capacity to produce higher strain and power than a rectangular cantilever beam. Rectangular cantilever beam has uneven strain distribution under load but trapezoidal cantilever beam produces almost even strain throughout the beam under load and increasing the power by 30% per unit volume (Baker 2005). Jin et al. (2017) introduced a truncated triangle beam, which can produce more power than trapezoidal and rectangular cantilever beam. Baker et al. (2005) analysed the variable thickness beam with a mass at the free end has the ability to increase harvester performance by a factor of 3.6 and its semi-analytical model was developed by Rayleigh–Ritz (R–R) method and validated using numerical simulations. Tapered cantilever beam with short wide beam has no significant effect on output power, but tapered with long slender has a positive effect on the performance of energy harvester (Matova et al. 2013). Hosseini and

✉ E. L. Pradeesh  
pradeesh.dmt@gmail.com  
S. Udhayakumar  
udhaya\_mech@yahoo.com

<sup>1</sup> Department of Mechanical Engineering, PSG College of Technology, Coimbatore, India

Hamed (2016a, b) developed analytical method to find the resonant frequency of V-shaped trapezoidal and triangular cantilever beam. By increasing the base of the V-shaped trapezoidal beam, the maximum resonant frequency could be achieved, which was calculated using the R–R method (Rouhollah Hosseini 2015). The same was analysed using numerical simulations (Hosseini and Hamed 2016c). Hosseini and Hamed (2015) introduced an analytical method to derive the output voltage of the V-shaped bimorph trapezoidal cantilever beam with uniform thickness. Hosseini and Nouri (2016) introduced optimization techniques to reduce the resonant frequency of V-shaped trapezoidal cantilever energy harvester. Zhou et al. (2018) analysed the effect of changing the length of piezoelectric material over the simply supported beam, from the experiment authors found that optimizing the length of piezoelectric material would improve the output of energy harvesting performance. Hosseini et al. (2018) studied the strain distribution over the rectangle, triangle and trapezoidal beam; from the finite element simulation, authors found that triangle beam produce two times more strain than rectangular cantilever beam. Goldschmidtboeing and Woias (2008) introduced curvature of homogeneity to the proof mass and found that shape of the beam has an only a slight effect on the energy harvesting performance but it has enormous influence on the excitation of amplitude and frequency. Salmani et al. (2015) derived an analytical expression for an exponentially tapered beam and the results were verified by comparing numerical with experimental methods. Hosseini et al. (2017a, b) derived an analytical solution to calculate the generated power of partially covered piezoelectric material on the cantilever beam. Paquin and St-Amant (2010) improved the performance of the energy harvester by varying the slope angle of the beam. From the experiment, authors found that the slope angle of  $0.94^\circ$  of the beam produce 71.94% more power compared to uniform thickness beam. Park et al. (2012) used MATLAB to optimize the geometry of energy harvester, which takes input from ANSYS. From the optimization, authors found that their optimum design could produce 160% more power than rectangular cantilever beam where rotary motion is used to excite the beam at the free end. Rosa and De Marqui Junior (2014) developed a mathematical model for tapered and reverse tapered beam and the model has a close agreement with experimental results. From the literature survey, it was found that the investigations on irregular geometries of beams are limited.

In this paper, the comparison is made between the various geometry of beam for energy harvesting by analysing the stress, strain, frequency response of the beam by analytical, numerical and experimental methods. The power generation of the proposed energy harvesters are discussed

by comparing voltage, power, frequency and input impedance.

## 2 Geometries of beam considered for energy harvester

The geometries of the beam considered for energy harvesting are Rectangle (REC), Triangle (TRI), Taper in width (TAP W), Taper in thick (TAP T), Taper in thick and width (TAP TW), Inverted taper in width (INTAP W), Inverted taper in thick and width (INTAP TW) are shown in Table 1.

### 2.1 Stress and strain analysis

The deformation of the piezoelectric material is based on the deformation of the cantilever beam, so it is essential to know the stress and strain of the beam. A 1 N of the load is applied at the free end. Aluminium is chosen as the material with a density of  $2700 \text{ kg/m}^3$  and Youngs modulus of 70 GPa.

The maximum stress  $\sigma$  of the cantilever beam was calculated using the bending moment Eq. (1).

$$\sigma = \frac{My}{I} = \frac{M}{I/y} \quad (1)$$

where  $M$  = bending moment,  $I$  = moment of inertia,  $y$  = distance of neutral axis from the surface.

The maximum strain  $\varepsilon$  of the cantilever beam can found by Eq. (2)

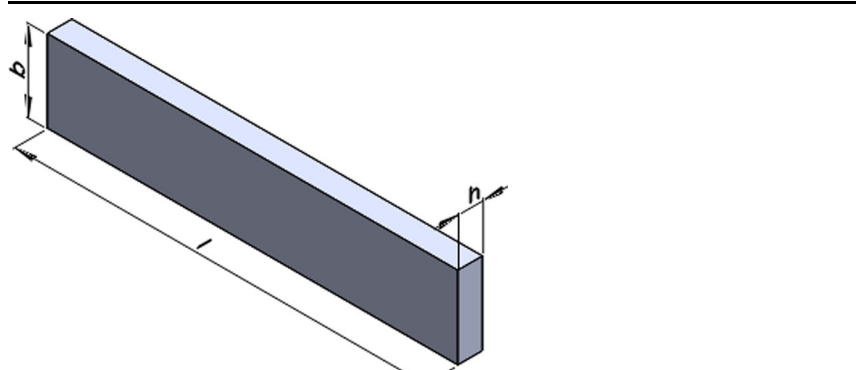
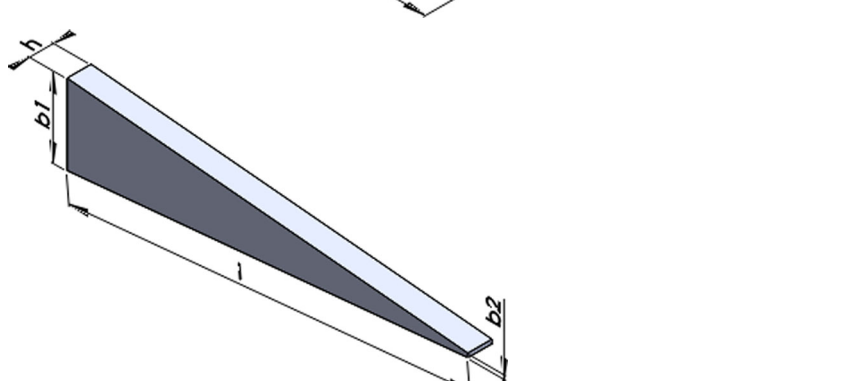
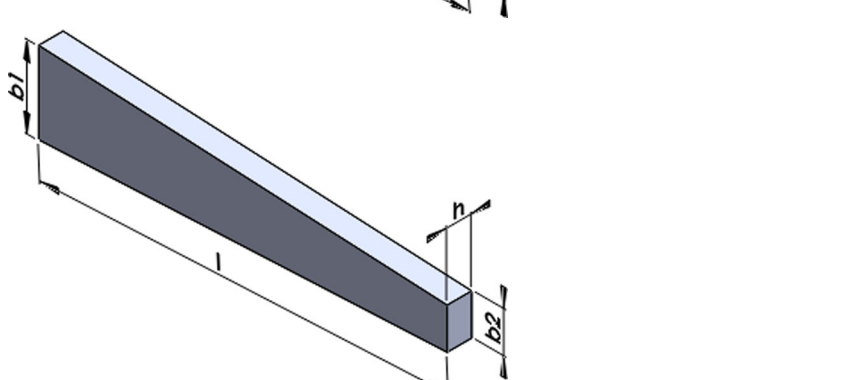
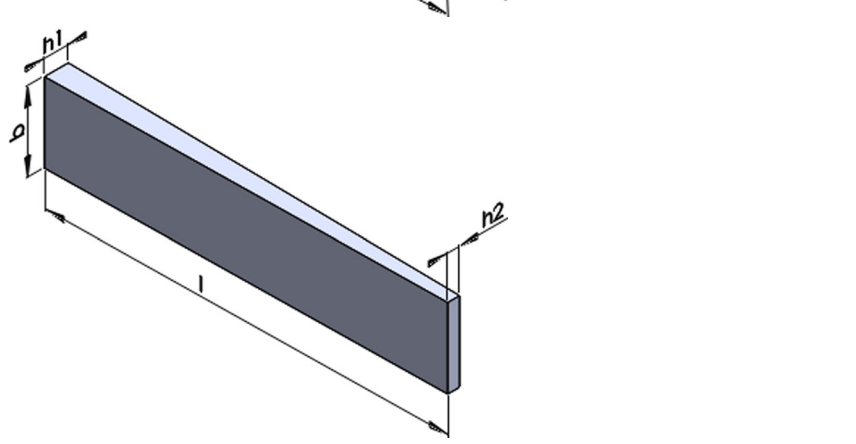
$$\varepsilon = \frac{\sigma}{E} \quad (2)$$

where  $E$  = Youngs Modulus.

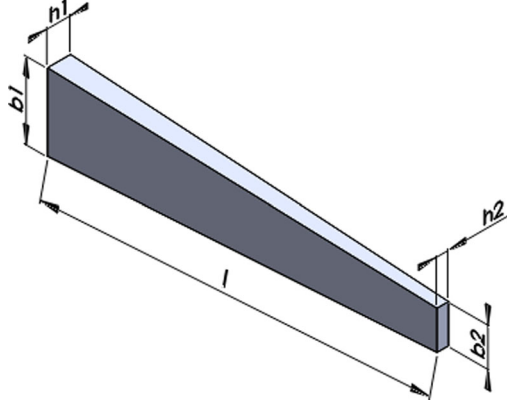
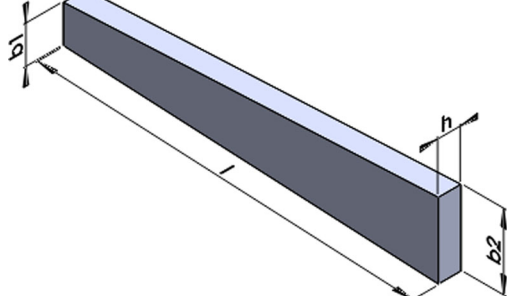
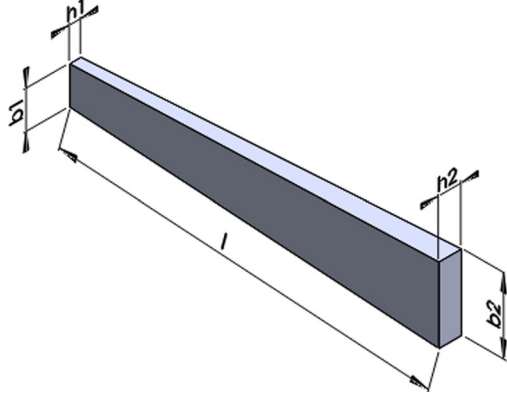
Using the above equations, the maximum stress and strain for the rectangular beam is analytically found to be  $60 \text{ N/mm}^2$  and  $8.57 \times 10^{-4}$  respectively.

The stress and strain for the rectangular beam was determined numerically using COMSOL Multiphysics 5.3a. Solid mechanics physics was used along with stationary study. Normal triangular mesh was used; the minimum and maximum element size were about 1.8–10 mm respectively. Figure 1 shows the maximum stress and strain of the rectangle cantilever beam. The maximum stress and strain of rectangular beam obtained analytically was in close agreement with the numerical result. Hence, the same methodology was followed for the numerical and analytical analysis of other beams considered in Sect. 2 and the results are tabulated in Table 2. The deviation between numerical and analytical methods are found to be very minimal.

**Table 1** Proposed geometries of energy harvester

Geometry	Nomenclature with dimensions Length(l) mm × width(b) mm × thick(h) mm
	<p>Rectangle (REC)  <math>l = 100</math>  <math>b = 10</math>  <math>h = 1</math></p>
	<p>Triangle (TRI)  <math>l = 100</math>  <math>b1 = 10</math>  <math>b2 = 0</math>  <math>h = 1</math></p>
	<p>Taper in width (TAP W)  <math>l = 100</math>  <math>b1 = 10</math>  <math>b2 = 5</math>  <math>h = 1</math></p>
	<p>Taper in thick (TAP T)  <math>l = 100</math>  <math>b = 10</math>  <math>h1 = 1</math>  <math>h2 = 0.5</math></p>

**Table 1** (continued)

Geometry	Nomenclature with dimensions Length( <i>l</i> ) mm × width( <i>b</i> ) mm × thick( <i>h</i> ) mm
	Taper in width and thick (TAP TW) $l = 100$ $b1 = 10$ $b2 = 5$ $h1 = 1$ $h2 = 0.5$
	Inverted taper in width (INTAP W) $l = 100$ $b1 = 5$ $b2 = 10$ $h = 1$
	Inverted taper in width and thick (INTAP TW) $l = 100$ $b1 = 5$ $b2 = 10$ $h1 = 0.5$ $h2 = 1$

From Table 2, it can be found that the maximum deviation between the analytical and numerical result is 2.42% only. The placement of piezoelectric material on the beam has the most influence on power production, so it is essential to know the strain over the length of the beam (Liao and Sodano 2012). Figure 2 shows the strain over the length of the beams under consideration which was obtained numerically through COMSOL Multiphysics 5.3a.

The strain over the length of the REC beam is constantly decreasing which is followed by TAP W and TAP T beam. The TRI beam produces almost constant strain over the

length of the beam. The strain produced in TAP TW and INTAP W beam is similar to TRI beam, but the amplitudes are higher. The INTAP TW beam produces higher strain near the fixed end compared to the other beams as shown in Fig. 2. This is due to more self-mass at free end and the strain concentration at the fixed end of the cantilever beam are induced by the inertial mass.

## 2.2 Frequency response of the beams

The piezoelectric energy harvesters are mostly used to power low power electronic devices and hence it is

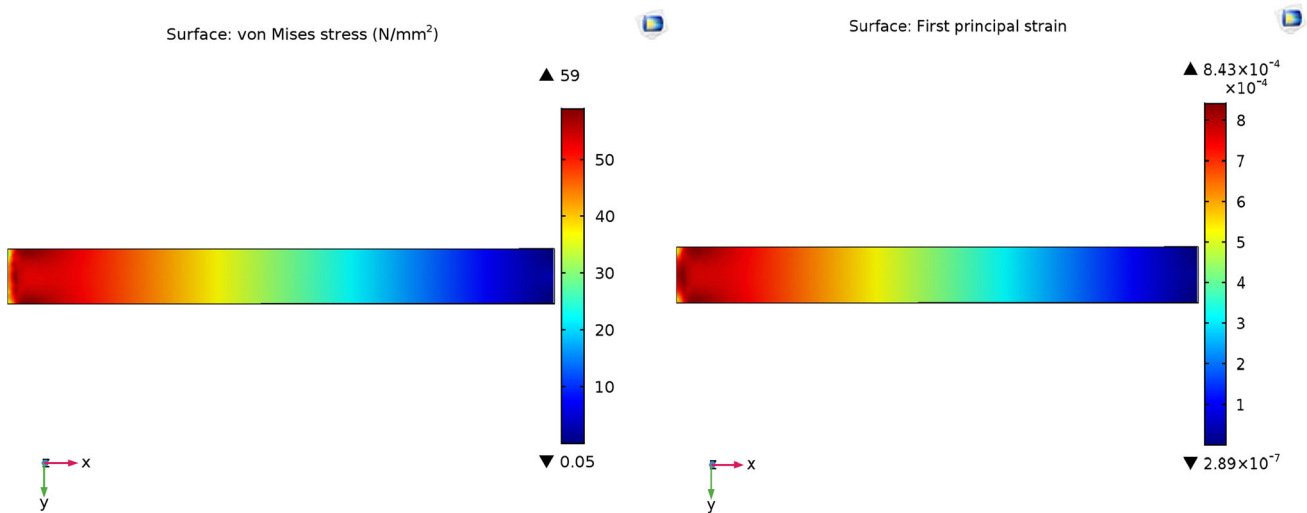


Fig. 1 Stress and strain of the rectangular cantilever beam

Table 2 Analytical and numerical value of stress and strain of the beam

Geometry of the beam	Volume (mm <sup>3</sup> )	Stress (N/mm <sup>2</sup> )		Deviation %	Strain (no unit)		Deviation %
		Analytical	Numerical		Analytical	Numerical	
REC	1000	60	59	0.01	8.57 E <sup>-4</sup>	8.43 E <sup>-4</sup>	0.01
TRI	500	60	60.6	0.01	8.57 E <sup>-4</sup>	8.46 E <sup>-4</sup>	0.01
TAP W	750	60	60	0	8.57 E <sup>-4</sup>	8.34 E <sup>-4</sup>	0.02
TAP T	750	60	61.3	0.02	8.57 E <sup>-4</sup>	8.53 E <sup>-4</sup>	0.01
TAP TW	583.3	71.1	71.4	0.01	1.01 E <sup>-3</sup>	1.02 E <sup>-3</sup>	0.01
INTAP W	750	115	115.9	0.77	1.65 E <sup>-3</sup>	1.61 E <sup>-3</sup>	2.42
INTAP TW	583.3	450	449	0.22	6.41 E <sup>-3</sup>	6.35 E <sup>-3</sup>	0.93

essential to produce high power at a lower frequency. It is difficult to analyse the frequency response of all the considered beams for energy harvesting by analytical and experimental methods. In order to validate the methodology of numerical analysis, two simple beams made of aluminium (Al) and copper (Cu) with the dimensions as shown in Table 3 were taken. The first mode of natural frequency was determined using analytical, numerical and experimental methods.

The deflection  $z(x)$  function of rectangular cantilever beam along the length of the beam can be calculated by Eq. (3) (Hosseini and Hamed 2016c)

$$z(x) = \frac{2Fx^2(3L_{bm} - x)}{E_{bm}W_{bm}T_{bm}^3} \tag{3}$$

where  $L_{bm}$ ,  $W_{bm}$ ,  $T_{bm}$  are the length, width and thickness of the cantilever beam as shown in Fig. 6.  $F$  force applied at the free end of the beam,  $E_{bm}$  Youngs modulus of the beam,  $x$  distance from the fixed end.

The Eq. (10) is used to find the resonance of the rectangular cantilever beam with the mass of the accelerometer.

If the cantilever beam is subjected to free vibration, then the system is to be considered as a continuous system in which the mass of the beam is considered as distributed along with stiffness of the beam. The equation of the motion can be written as (Hosseini and Hamed 2016c).

$$\frac{d^2y}{dx^2} \left\{ EI(x) \frac{d^2y(x)}{dx^2} \right\} = \omega^2 m(x) Y(x) \tag{4}$$

where  $E$  Young’s modulus,  $I$  moment of inertia,  $Y(x)$  displacement in  $y$  direction at the distance of  $x$ .  $\omega$  natural frequency of the beam,  $x$  distance from fixed end,  $m$  mass per unit length,  $m = \rho A(x)$ ,  $\rho$  the density of the material.

The natural frequency  $\omega$  of the cantilever beam from the equation of motion is given by (Khurmi and Gupta 2005)

**Fig. 2** Strain over the length of the proposed beams

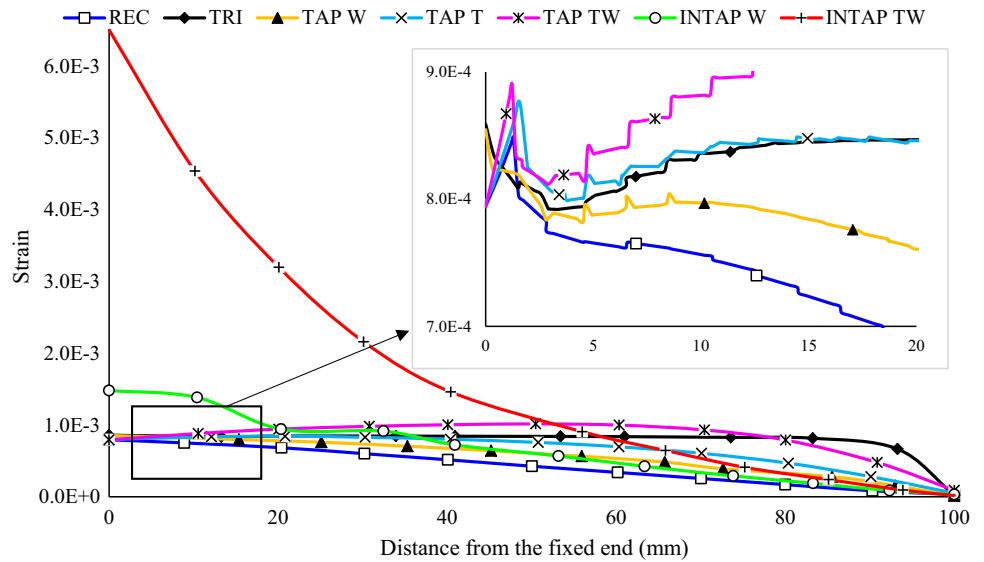


**Table 3** Dimensions and properties of Al and Cu beam

Material	Dimension $l \times b \times h$ (mm <sup>3</sup> )	Density (kg/m <sup>3</sup> )	Youngs modulus (GPa)
Aluminium	150 × 49.73 × 3.05	2700	68.9
Copper	121 × 23.4 × 0.51	8900	110

$$\omega = \alpha_n^2 \sqrt{\frac{EI}{mL^3}} = \alpha_n^2 \sqrt{\frac{EI}{\rho AL^4}} \tag{5}$$

where  $\alpha_n = 1.875$ .

The natural frequency of the cantilever beam with the mass of the accelerometer  $\omega_a$  can be written as

$$\omega_a = \sqrt{\frac{k}{m_{eff}}} \tag{6}$$

with  $k = \frac{3EI}{L^3}$ .

Here the beam is considered as mass-less with stiffness  $k$ ,  $m_{eff}$  discrete effective mass at the free end, which produces the frequency as a continuous beam without tip mass.

From which effective mass at the tip is given by

$$m_{eff} = \frac{3EI}{L^3 \omega_a^2} \tag{7}$$

$$\text{with } \omega_a = 1.875^2 \sqrt{\frac{EI}{\rho AL^4}} = 1.875^2 \sqrt{\frac{EI}{mL^3}}$$

$$m_{eff} = \frac{3EI}{L^3} \frac{mL^3}{1.875^4 EI} = \frac{3}{12.359} m = \frac{33}{140} m. \tag{8}$$

By considering, the mass of accelerometer  $m_{acc}$  at the free end of the beam and then the total mass  $M_T$  at the free end will be

$$M_T = m_{eff} + m_{acc}. \tag{9}$$

The natural frequency of the discrete beam after considering the mass of the accelerometer can be written as

$$\omega_a = \sqrt{\frac{k}{M_T}} = \sqrt{\frac{3EI}{L^3 M_T}}. \tag{10}$$

The analytical result for the first natural frequency of Al and Cu beam with the mass of the accelerometer using the equations was shown in Table 4.

The numerical analysis was done through COMSOL Multiphysics 5.3a. The first mode was found using Eigen frequency study. The boundary conditions were the same as in stress and strain analysis in Sect. 2.1. The tip mass considered was the mass of the accelerometer, which is about 0.001 kg. Figure 3 shows the first mode of Al and Cu beam with mass of the accelerometer, which are 107.16 Hz and 17.261 Hz respectively.

### 2.3 Experimental setup

The following experimental setup was used to determine the first mode of the beam experimentally. An electrodynamic shaker with the control unit as shown in Fig. 4 is used to provide the base excitation in a sine wave to the beam. LabVIEW software is interfaced with NI DAQ 9234 along with an accelerometer (PCB-356A01) that is placed on the beam to determine the vibrating frequency of the beam.

**Table 4** Frequency response of aluminium and copper beam

Beam	1st mode (Hz) with tip mass		
	Analytical	Numerical	Experimental
Aluminium	108.55	107.16	108.54
Copper	17.40	17.26	16.98

The experimental results for Al and Cu beam using LabVIEW is plotted in Fig. 5, which shows the resonant frequency of Al and Cu beams in first mode. The numerical result has good agreement with analytical and experimental results as shown in Table 4. Hence, the same methodology was applied for numerical analysis of the beams considered in Sect. 2 to determine the first mode.

The first mode of natural frequency for the considered beams of energy harvesting were obtained numerically, which is shown in Table 5.

From Table 5, it could be found that INTAP TW beam reaches resonance at a lower frequency, which is followed by INTAP W, REC, TAP T, TAP W, TAP TW and TRI. The variation in frequency of the beams are based on the stiffness and mass of the beam.

### 3 Power generation of piezoelectric materials

The next step is to determine the power generation of piezoelectric materials for considered beams. The dimensions of the considered beam for energy harvesting are tabulated in Table 6. Figure 6 shows the rectangle cantilever beam with a piezoelectric material. The size of the Lead Zirconate Titanate-5A (PZT-5A) is 10 mm in length, 10 mm in width and 0.5 mm in thick respectively. The

PZT-5A is placed near to the fixed end of the beam as shown in Fig. 6.

The aluminium is chosen as the substrate. The material properties of Al and PZT-5a are shown in Table 7.

The analytical Eq. (11) used to calculate the generated open circuit (OC) voltage from a rectangular cantilever piezoelectric energy harvester.

The voltage generated by the piezoelectric material can be calculated by Eq. (11) (IEEE 1996)

$$V = g_{31}T_{pz}\sigma_{pz} \tag{11}$$

where  $V$  is the voltage generated by a piezoelectric material,  $g_{31}$  is the piezoelectric coefficient,  $T_{pz}$  is the thickness of the piezoelectric material,  $\sigma_{pz}$  applied stress on the piezoelectric material during poling.

When the piezoelectric material and substrate are subjected to external force, the induced piezoelectric material strain  $\epsilon_{pz}$  can be expressed as (Eggborn 2003; Nabavi and Zhang 2017)

$$\epsilon_{pz} = \frac{\sigma_{pz}}{E_{pz}} \tag{12}$$

$$\sigma_{pz} = \epsilon_{pz}E_{pz} \tag{13}$$

where  $E_{pz}$  is the Youngs modulus of the piezoelectric material.

The average strain on the piezoelectric material and the top surface of the beam can be written as (Eggborn 2003)

$$\epsilon_{pz} = -\frac{6ME_{bm}T_{bm}(T_{pz} + T_{bm})}{W_{pz}[E_{pz}^2T_{pz}^4 + E_{bm}^2T_{bm}^4 + 2E_{pz}T_{pz}E_{bm}T_{bm}(2T_{pz}^2 + 3T_{pz}T_{bm} + 2T_{bm}^2)]} \tag{14}$$

where  $M$  is the actuating momentum,  $E_{bm}$  is the Youngs modulus of the beam,  $T_{bm}$  is the thickness of the beam,  $T_{pz}$  is the thickness of the piezoelectric material,  $W_{pz}$  is the width of the piezoelectric material.

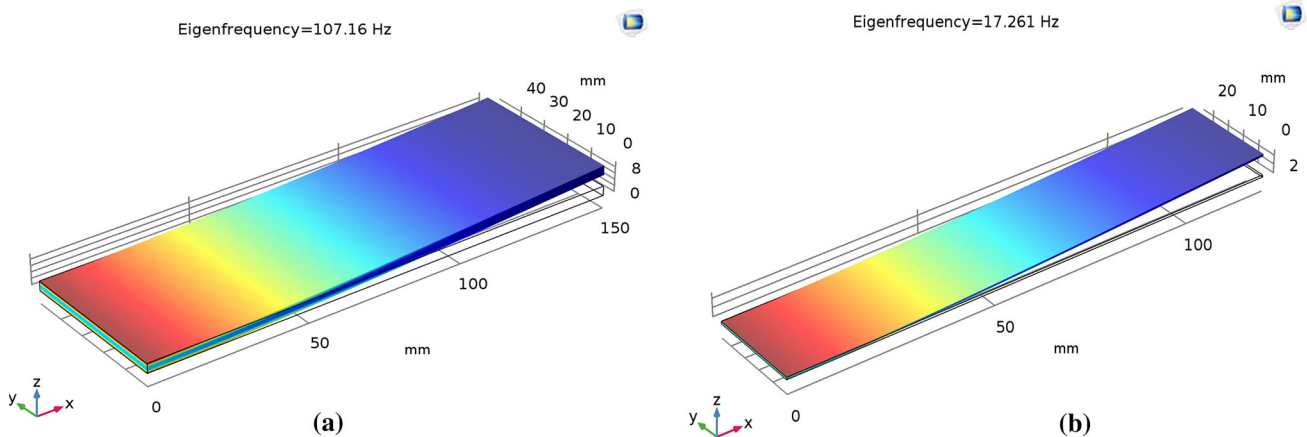


**Fig. 3** First mode of the Al and Cu beam using numerical method. **a** Al beam. **b** Cu beam

**Fig. 4** Experimental setup used to find the first mode of the Al and Cu beam

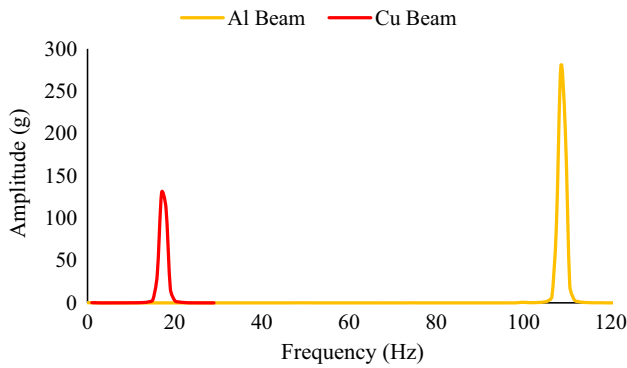
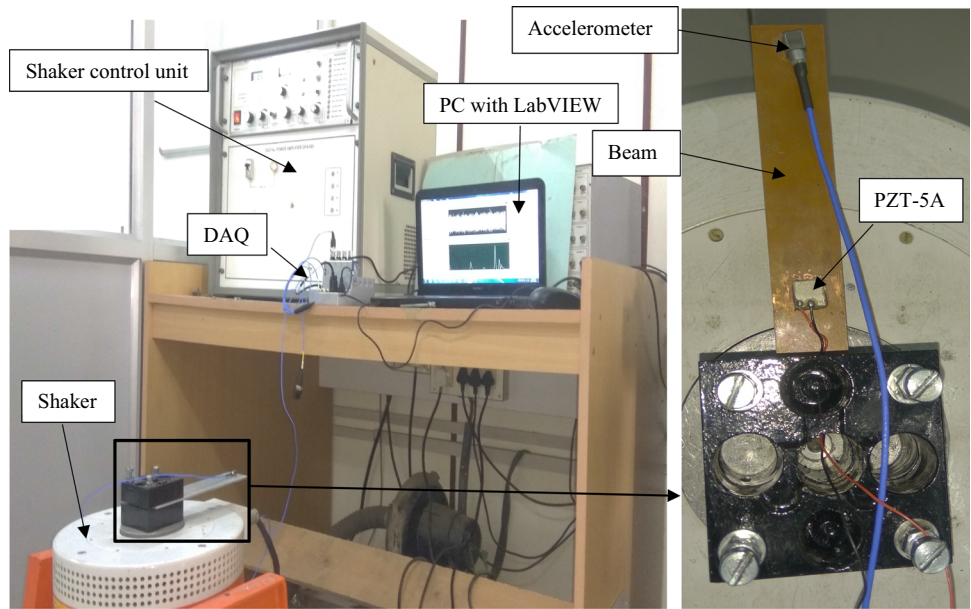


**Fig. 5** Experimental result for first mode of Al and Cu beams

The actuating momentum  $M$  of the piezoelectric energy harvester can be found by

$$M = E_{bm} \times I_{bm} \times R \tag{15}$$

where  $I$  moment of inertia,  $R$  radius of curvature, which can be found by Macaulay’s method (Timoshenko 1940)

$$R = \frac{1}{E_{bm} \times I_{bm} \times L_{pz}} \times (\rho_{pz} \times g \times vol_{pz}) \times \left( \frac{L_{pz}^2}{2} - \frac{(L_{pz} - a)^3}{6} - \frac{(L_{pz} - b)^3}{6} \right) \tag{16}$$

where  $L_{pz}$  length of the piezoelectric material,  $\rho_{pz}$  density of piezoelectric material,  $g$  gravity,  $vol_{pz}$  volume of piezoelectric material,  $a$  distance of starting of piezoelectric material from the fixed end of the beam,  $b$  distance of ending of piezoelectric material from the fixed end of the beam as shown in Fig. 6.

**Table 5** First mode for the considered beams of energy harvesting

Type of the beam	First mode (Hz)
REC	83.0
TRI	168.7
TAP W	101.8
TAP T	90.0
TAP TW	108.8
INTAP W	66.8
INTAP TW	30.6

The actuating momentum  $M$  can be calculated by substituting (16) in (15)

$$M = E_{bm} \times I_{bm} \times \frac{1}{E_{bm} \times I_{bm} \times L_{pz}} \times (\rho_{pz} \times g \times vol_{pz}) \times \left( \frac{L_{pz}^2}{2} - \frac{(L_{pz} - a)^3}{6} - \frac{(L_{pz} - b)^3}{6} \right) \tag{17}$$

$$M = \frac{1}{L_{pz}} \times (\rho_{pz} \times g \times vol_{pz}) \times \left( \frac{L_{pz}^2}{2} - \frac{(L_{pz} - a)^3}{6} - \frac{(L_{pz} - b)^3}{6} \right) \tag{18}$$

The generated OC voltage can be calculated by combining (14) and (13) in (11)

$$V = - \frac{6Mg_{31}T_{pz}E_{pz}E_{bm}T_{bm}(T_{bm} + T_{pz})}{W_{pz}[E_{pz}^2T_{pz}^4 + E_{bm}^2T_{bm}^4 + 2E_{pz}T_{pz}E_{bm}T_{bm}(2T_{pz}^2 + 3T_{pz}T_{bm} + 2T_{bm}^2)]} \tag{19}$$



**Table 6** Dimensions of the considered beam for energy harvesting

Type	Dimension (mm <sup>3</sup> ) Length(l) × width(b) × thick(h)
REC	100 × 10 × 1
TRI	100 × 12–0 × 1
TAP W	100 × 11–5 × 1
TAP T	100 × 10 × 1–0.5
TAP TW	100 × 11–5 × 1–0.5
INTAP W	100 × 10–15 × 1
INTAP TW	100 × 10–15 × 0.5–1

The generated OC voltage can also be written as

$$V = - \frac{6Mg_{31}J(1 + K)}{W_{pz} \times T_{pz}[1 + J^2K^2 + 2J(2 + 3K + 2K^2)]} \quad (20)$$

where  $J = \frac{E_{bm}T_{bm}}{E_{pz}T_{pz}}$ ,  $K = \frac{T_{bm}}{T_{pz}}$ .

Using the above equations, the OC voltage generated for rectangular beam is found to be 25.92 V and it is shown in Table 8.

For numerical study, solid mechanics, electrostatics and electrical circuit are the physics used along with the frequency domain study in COMSOL Multiphysics 5.3a. 1 g of body load is applied to energy harvester. The isotropic mechanical damping loss factor of 5% was considered for beam and PZT-5A. The model were run for different mesh types with minimum and maximum element size for coarse

(2.8–15 mm), normal (1.8–10 mm), fine (1–8 mm) and finer (0.4–5.5 mm). From the different mesh analysis, it was found that normal triangular mesh produce better result at less time step along with the step frequency of 0.25 Hz.

The numerical result of OC voltage for REC cantilever energy harvester is shown in Table 8. The numerical result is in close agreement with the analytical result with a deviation of 7.9%. The same numerical methodology was applied to other energy harvesters. Figure 7 shows the open circuit peak-to-peak (p–p) voltage of different energy harvesters obtained numerically.

From Fig. 7, it can be seen that INTAP TW produces more voltage at a lower frequency, which is followed by INTAP W, REC, TAP T, TAP W, TAP TW, TRI. From this, it can be found that the peak OC voltage at the resonant frequency for different energy harvester. The resonant frequency for energy harvesters are used to find the optimum load. The maximum power transfer could be achieved by a piezoelectric material when the optimum load is matched with the energy harvesters internal impedance. The optimum load was found by keeping the resonant frequency constant for different beams and the auxiliary sweep was made with different load resistance in COMSOL Multiphysics 5.3a. Figure 8 shows the characteristics of power (P) with respect to the different load resistance varying from 10 kΩ to 10 MΩ.

**Fig. 6** Rectangle beam with the piezoelectric material

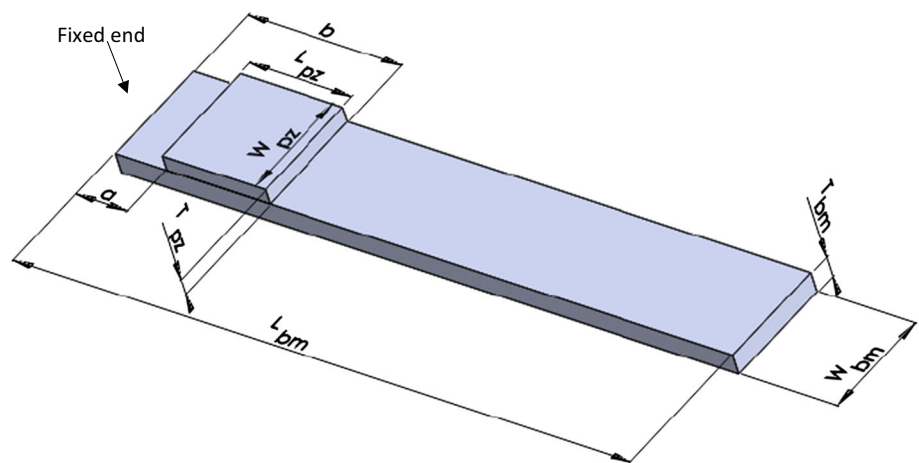


**Table 7** Material properties of Al and PZT-5A

Properties	PZT-5A	Aluminium
Young's modulus (GPa)	61	70
Density (kg/m <sup>3</sup> )	7750	2700
Piezoelectric coefficient, g <sub>31</sub> (× 10 <sup>-3</sup> Vm/N)	- 11	-
Piezoelectric constant (C/m <sup>2</sup> )	- 5.7	-

**Table 8** Analytical and numerical comparison of open circuit voltage

Energy harvester	Analytical	Numerical	Deviation %
REC beam	25.92 V <sub>p-p</sub>	23.85 V <sub>p-p</sub>	7.9

Figure 8 shows the INTAP TW and TAP W beam produce 0.7 and 0.07 mW of maximum power at 1 MΩ. INTAP W, REC, TAP T and TAP WT beam produce 0.6, 0.3, 0.1 and 0.09 mW of maximum power at 0.56 MΩ. The TRI beam produce 0.1 mW of maximum power at 0.31 MΩ.

The maximum power *P*, generated by the piezoelectric energy harvester can be determined by (Rami Reddy et al. 2016)

$$P = \frac{V^2}{4R_L} \tag{21}$$

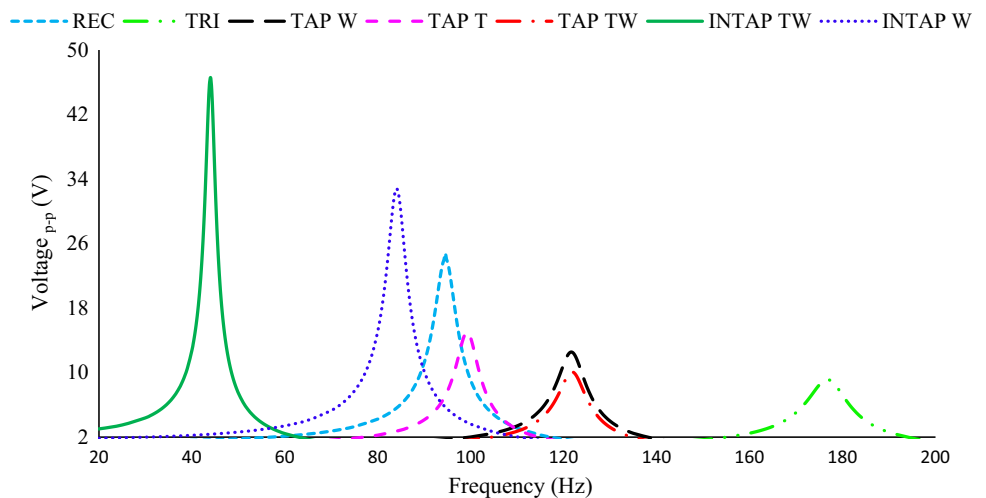
where  $R_L = \frac{1}{\omega C_v}$  is the impedance of the piezoelectric material,  $\omega$  is the natural frequency,  $C_v$  is the capacitance of the piezoelectric material.

From the auxiliary sweep of load resistance, the optimum load was calculated for each energy harvester. Figures 9 and 10 show the voltage and power obtained numerically with respect to frequency under the optimum load.

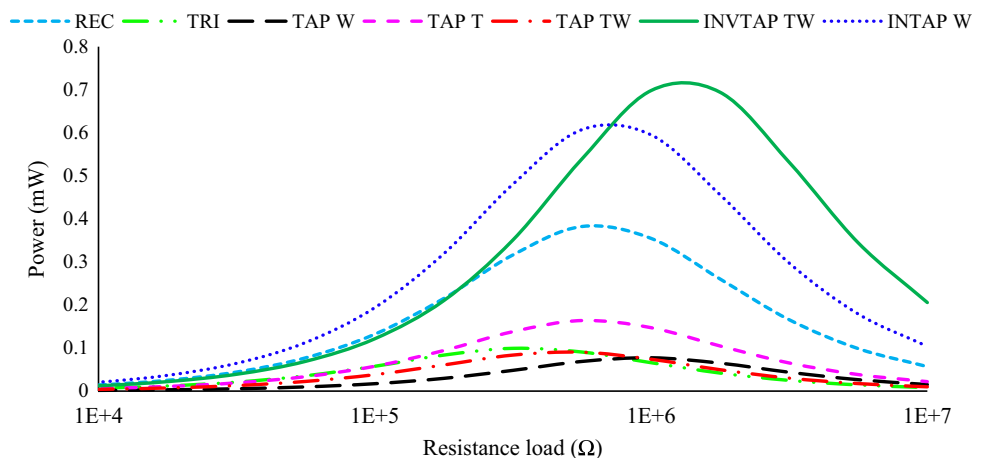
Figure 9 shows INTAP TW and INTAP W beam produce 44.3 and 20.5% more voltage than REC beam. TAP T, TAP W, TAP TW, TRI beam produce 34.6, 40.2, 51.5 and 61.7% less voltage than REC beam, which are shown in Table 9.

Figure 10 shows INTAP TW and INTAP W beam produce 45.14 and 37% more power than REC beam. TAP T, TRI, TAP TW, TAP W beam produce 57.2, 73.9, 76.5 and 80% less power than REC beam. The operating range of energy harvesters are REC (72–115 Hz), TRI (115–196 Hz), TAP W (109–133 Hz), TAP T (83–112 Hz), TAP TW (108–133 Hz), INTAP W

**Fig. 7** Frequency vs open circuit voltage



**Fig. 8** Load resistance vs power



**Fig. 9** Frequency vs voltage under optimum load

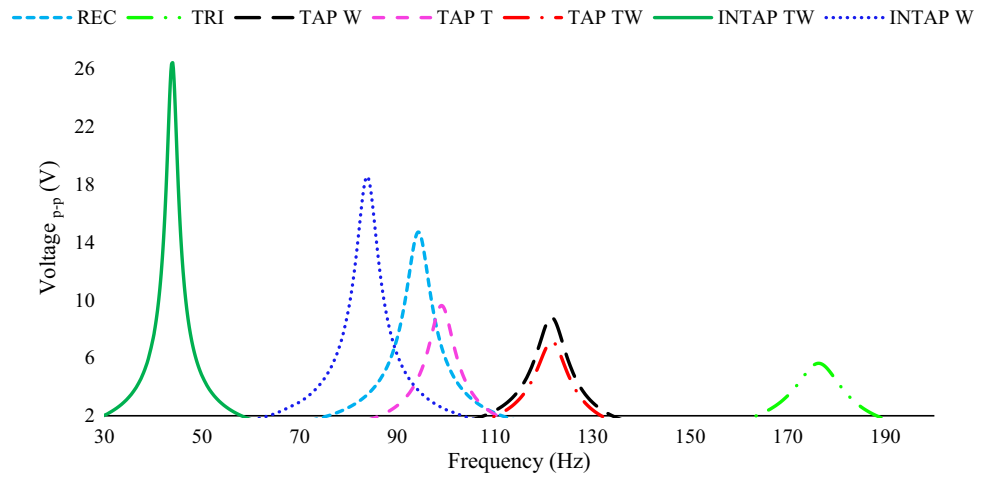


**Fig. 10** Frequency vs power under optimum load

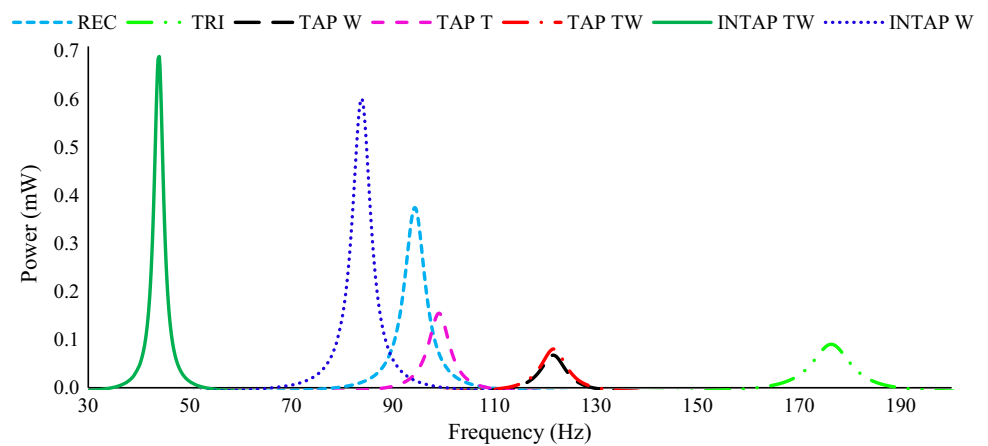


**Table 9** Voltage and power characteristics under the optimum load

Beam	Volume (mm <sup>3</sup> )	Frequency (Hz)	Optimum load (M Ω)	Voltage (V)	Power (mW)	P/mm <sup>3</sup> (μW)
REC	1000	94.25	0.563	14.71	0.384	0.384
TRI	625	176.25	0.316	5.63	0.100	0.160
TAP W	800	121.5	1	8.80	0.077	0.096
TAP T	750	99	0.562	9.62	0.164	0.210
TAP TW	625	121.75	0.562	7.13	0.090	0.144
INTAP W	1250	83.75	0.563	18.50	0.610	0.488
INTAP TW	958.33	44	1	26.42	0.700	0.730

(60–107 Hz), INTAP TW (31–57 Hz). In the above said operating range, each energy harvester can produce minimum output power of 5 μW. The voltage and power characteristics with respect to frequency under the optimum load are shown in Table 9.

In the considered beams of piezoelectric energy harvester, INTAP TW and INTAP W beam produce 47.39 and 21.31% more power per unit volume than REC beam. TAP T, TRI, TAP TW and TAP W beam produce 45.31, 58.3,

62.5 and 75% less power per unit volume than REC beam. The excitation frequency of INTAP TW and INTAP W is 53.3 and 11.1% less than REC beam. TAP T, TAP W, TAP TW and TRI beam have 4.7, 22.4, 22.5 and 46.5% more than REC beam.

## 4 Conclusion

- Various geometries of beams were considered for energy harvester.
- The stress and strain analysis of various geometries of piezoelectric energy harvesters were analytically and numerically discussed. The INTAP TW and INTAP W beam produce more strain at the fixed end compared to other beams.
- The frequency response of the considered beams were numerically analysed. The INTAP TW beam reaches resonance at a 53.3% lower frequency than the REC beam.
- Optimum load was determined using auxiliary sweep in COMSOL Multiphysics. By placing the optimum load maximum power generation could be achieved at the resonance frequency. INTAP TW beam produced 47.39% more power per unit volume at a lower frequency than the REC beam.
- Among the proposed piezoelectric energy harvester, INTAP TW piezoelectric energy harvester has the ability to produce more power at the lower excitation frequency.

## References

- Baker J (2005) Alternative geometries for increasing power density in vibration energy scavenging. In: 3rd international energy conversion engineering conference 15–18 August 2005, San Fr Calif 1–12. <https://doi.org/10.2514/6.2005-5617>
- Baker J, Roundy S, Wright P (2005) Alternative geometries for increasing power density in vibration energy scavenging for wireless sensor networks. 3rd international energy conversion engineering conference 15–18 August 2005, San Francisco, California. American Institute of Aeronautics and Astronautics, Reston, pp 1–12
- Chandrakasan A, Amirtharajah R, Goodman J, Rabiner W (1998) Trends in low power digital signal processing. In IEEE, pp 604–607
- Damya A, AbbaspourSani E, Rezazadeh G (2018) An innovative piezoelectric energy harvester using clamped–clamped beam with proof mass for WSN applications. *Microsyst Technol* 1:1–9. <https://doi.org/10.1007/s00542-018-3890-6>
- Eggorn T (2003) Analytical models to predict power harvesting with piezoelectric materials. Polytechnic Institute and State University, Blacksburg
- Goldschmidtboeing F, Woias P (2008) Characterization of different beam shapes for piezoelectric energy harvesting. *J Micromech Microeng* 18:104013. <https://doi.org/10.1088/0960-1317/18/10/104013>
- Hosseini R, Hamed M (2015) Improvements in energy harvesting capabilities by using different shapes of piezoelectric bimorphs. *J Micromech Microeng* 25:125008. <https://doi.org/10.1088/0960-1317/25/12/125008>
- Hosseini R, Hamed M (2016a) An investigation into resonant frequency of triangular V-shaped cantilever piezoelectric vibration energy harvester. *J Solid Mech* 8:560–567
- Hosseini R, Hamed M (2016b) Resonant frequency of bimorph triangular V-shaped piezoelectric cantilever energy harvester. *J Comput Appl Res Mech Eng* 6:65–73. <https://doi.org/10.22061/JCARME.2016.521>
- Hosseini R, Hamed M (2016c) An investigation into resonant frequency of trapezoidal V-shaped cantilever piezoelectric energy harvester. *Microsyst Technol* 22:1127–1134. <https://doi.org/10.1007/s00542-015-2583-7>
- Hosseini R, Nouri M (2016) Shape design optimization of unimorph piezoelectric cantilever energy harvester. *J Solid Mech* 47:247–259. <https://doi.org/10.22059/JCAMECH.2017.224975.126>
- Hosseini R, Hamed M, Ebrahimi Mamaghani A et al (2017a) Parameter identification of partially covered piezoelectric cantilever power scavenger based on the coupled distributed parameter solution. *Int J Smart Nano Mater* 8:110–124. <https://doi.org/10.1080/19475411.2017.1343754>
- Hosseini R, Hamed M, Im J et al (2017b) Analytical and experimental investigation of partially covered piezoelectric cantilever energy harvester. *Int J Precis Eng Manuf* 18:415–424. <https://doi.org/10.1007/s12541-017-0050-3>
- Hosseini R, Zargar O, Hamed M (2018) Improving power density of piezoelectric vibration-based energy scavengers. *J Solid Mech* 10:98–109
- IEEE (1996) Publication and Proposed Revision of ANSI/IEEE Standard 176–1987 “ANSI/IEEE Standard on Piezoelectricity”. *IEEE Trans Ultrason Ferroelectr Freq Control* 43:717. <https://doi.org/10.1109/TUFFC.1996.535477>
- Jin L, Gao S, Zhou X, Zhang G (2017) The effect of different shapes of cantilever beam in piezoelectric energy harvesters on their electrical output. *Microsyst Technol* 23:4805–4814. <https://doi.org/10.1007/s00542-016-3261-0>
- Khurmi RS, Gupta JK (2005) *Theory of machines*. Eurasia Publishing House, New Delhi
- Kim S, Clark WW, Wang Q-M (2005) Piezoelectric energy harvesting with a clamped circular plate: experimental study. *J Intell Mater Syst Struct* 16:855–863. <https://doi.org/10.1177/1045389X05054043>
- Liao Y, Sodano HA (2012) Optimal placement of piezoelectric material on a cantilever beam for maximum piezoelectric damping and power harvesting efficiency. *Smart Mater Struct* 21:105014. <https://doi.org/10.1088/0964-1726/21/10/105014>
- Mateu L, Moll F (2005) Optimum piezoelectric bending beam structures for energy harvesting using shoe inserts. *J Intell Mater Syst Struct* 16:835–845. <https://doi.org/10.1177/1045389X05055280>
- Matova SP, Renaud M, Jambunathan M et al (2013) Effect of length/width ratio of tapered beams on the performance of piezoelectric energy harvesters. *Smart Mater Struct* 22:1–8. <https://doi.org/10.1088/0964-1726/22/7/075015>
- Md Ralib AA, Nordin AN, Othman R, Salleh H (2011) Design, simulation and fabrication of piezoelectric micro generators for aero acoustic applications. *Microsyst Technol* 17:563–573. <https://doi.org/10.1007/s00542-011-1228-8>
- Mossi K, Green C, Ounaies Z, Hughes E (2005) Harvesting energy using a thin unimorph prestressed bender: geometrical effects. *J Intell Mater Syst Struct* 16:249–261. <https://doi.org/10.1177/1045389X05050008>
- Nabavi S, Zhang L (2017) Design and optimization of piezoelectric MEMS vibration energy harvesters based on genetic algorithm. *IEEE Sens J* 17:7372–7382. <https://doi.org/10.1109/JSEN.2017.2756921>

- Paquin S, St-Amant Y (2010) Improving the performance of a piezoelectric energy harvester using a variable thickness beam. *Smart Mater Struct* 19:105020. <https://doi.org/10.1088/0964-1726/19/10/105020>
- Park J, Lee S, Kwak BM (2012) Design optimization of piezoelectric energy harvester subject to tip excitation. *J Mech Sci Technol* 26:137–143. <https://doi.org/10.1007/s12206-011-0910-1>
- Rami Reddy A, Umapathy M, Ezhilarasi D, Gandhi U (2016) Improved energy harvesting from vibration by introducing cavity in a cantilever beam. *J Vib Control* 22:3057–3066. <https://doi.org/10.1177/1077546314558498>
- Rosa M, De Marqui Junior C (2014) Modeling and analysis of a piezoelectric energy harvester with varying cross-sectional area. *Shock Vib* 2014:1–9. <https://doi.org/10.1155/2014/930503>
- Rouhollah Hosseini MH (2015) Study of the resonant frequency of unimorph triangular V-shaped piezoelectric cantilever energy harvester. *Int J Adv Des Manuf Technol* 8(75):82
- Roundy S, Wright PK (2004) A piezoelectric vibration based generator for wireless electronics. *Smart Mater Struct* 13:1131–1142. <https://doi.org/10.1088/0964-1726/13/5/018>
- Roundy S, Wright PK, Rabaey J (2003) A study of low level vibrations as a power source for wireless sensor nodes. *Comput Commun* 26:1131–1144. [https://doi.org/10.1016/S0140-3664\(02\)00248-7](https://doi.org/10.1016/S0140-3664(02)00248-7)
- Salmani H, Rahimi GH, Kordkheili SAH (2015) An exact analytical solution to exponentially tapered piezoelectric energy harvester. *Shock Vib* 2015:1–13
- Timoshenko S (1940) *Strength of materials part 1*, 2nd edn. D. Van Nostrand Co., Inc, Princeton
- Zhou X, Gao S, Jin L et al (2018) Effects of changing PZT length on the performance of doubly-clamped piezoelectric energy harvester with different beam shapes under stochastic excitation. *Microsyst Technol* 24:3799–3813. <https://doi.org/10.1007/s00542-018-3845-y>

**Publisher's Note** Springer Nature remains neutral with regard to jurisdictional claims in published maps and institutional affiliations.